X-, γ-ray and Neutron Production in Solar Flares

R. J. Murphy, J. M. Ryan, M. Pesce-Rollins & G. H. Share

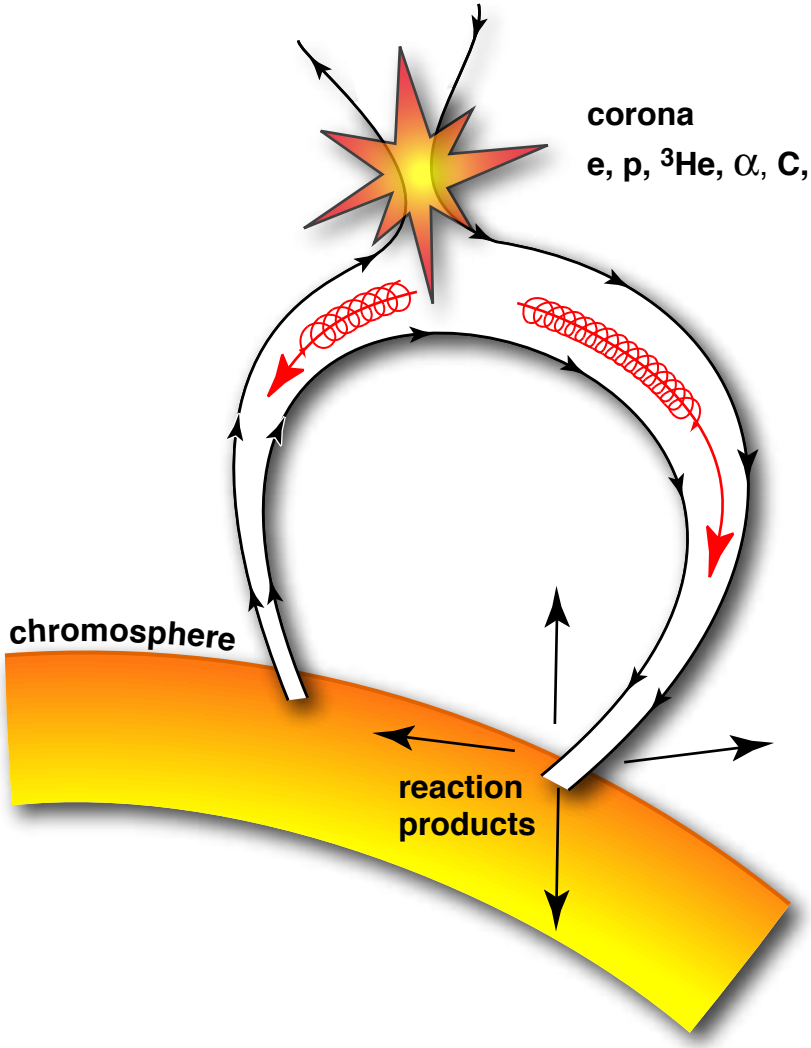

e^-: X- and γ-ray bremsstrahlung

ions: excited nuclei → prompt γ-ray line radiation

neutrons → { escape to space ; capture on H → 2.223 MeV γ-ray line

radioactive nuclei → { delayed γ-ray line emission ; $e^+ \rightarrow \gamma_{511}$

$\pi \rightarrow \gamma$ (decay, $e^{\pm}$ bremsstrahlung, γ_{511})

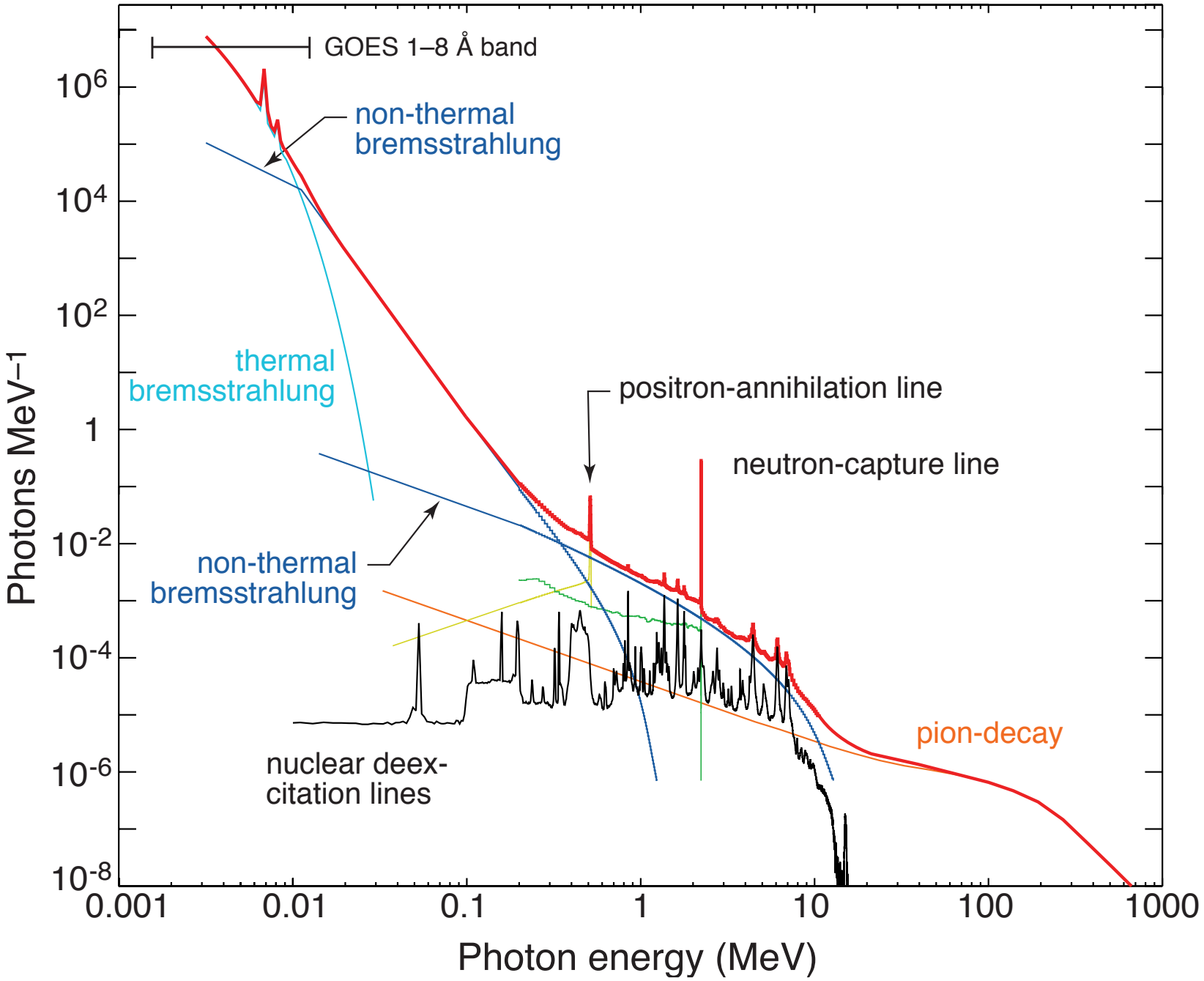
GOES 1–8 Å band
non-thermal
bremsstrahlung
thermal
bremsstrahlung
positron-annihilation line
neutron-capture line
non-thermal
bremsstrahlung
nuclear deex-
citation lines
pion-decay
Photons MeV–1
Photon energy (MeV)
10^6
10^4
10^2
1
10^-2
10^-4
10^-6
10^-8
0.001
0.01
0.1
1
10
100
1000

- What are the accelerated-ion and ambient compositions? What is the association between flare-accelerated ions and ^{3}He-rich SEP event ions? Is FIP fractionation taking place at the chromospheric densities where flare ions are interacting?

- What is the angular distribution of interacting flare ions? What can be learned about accelerated-ion transport?

- What is the shape of the 511 keV positron annihilation-line and what can it reveal about flare conditions at the Sun?

- Can long-lived radioactive isotope deexcitation lines be observed? Can they reveal small-scale or continuous ion acceleration? What do they say about atmospheric mixing?

- What is the association of Fermi high-energy emission and SEPs? What improvment in PSF at 100's of MeV will help resolve the issue?

- What unique information do observations of flare-produced neutrons provide?

- How efficient and how fast is primary flare electron acceleration? To what energies are electrons accelerated?

Ambient and Accelerated-Ion Composition

Interactions of flare-accelerated ions with the solar atmosphere produce gamma-ray deexcitation lines.

$$\left.\begin{matrix} p \\ \alpha \\ {}^{3}He \end{matrix}\right\} + {}^{12}C \longrightarrow {}^{12}C^{*}4.439$$

Narrow line ratios are proportional to the relative abundances of the chromosphere where the ions interact

$${}^{12}C + \left\{\begin{matrix} H \\ {}^{4}He \end{matrix}\right. \longrightarrow {}^{12}C^{*}4.439$$

Broad line ratios are proportional to the relative abundances of the accelerated ions

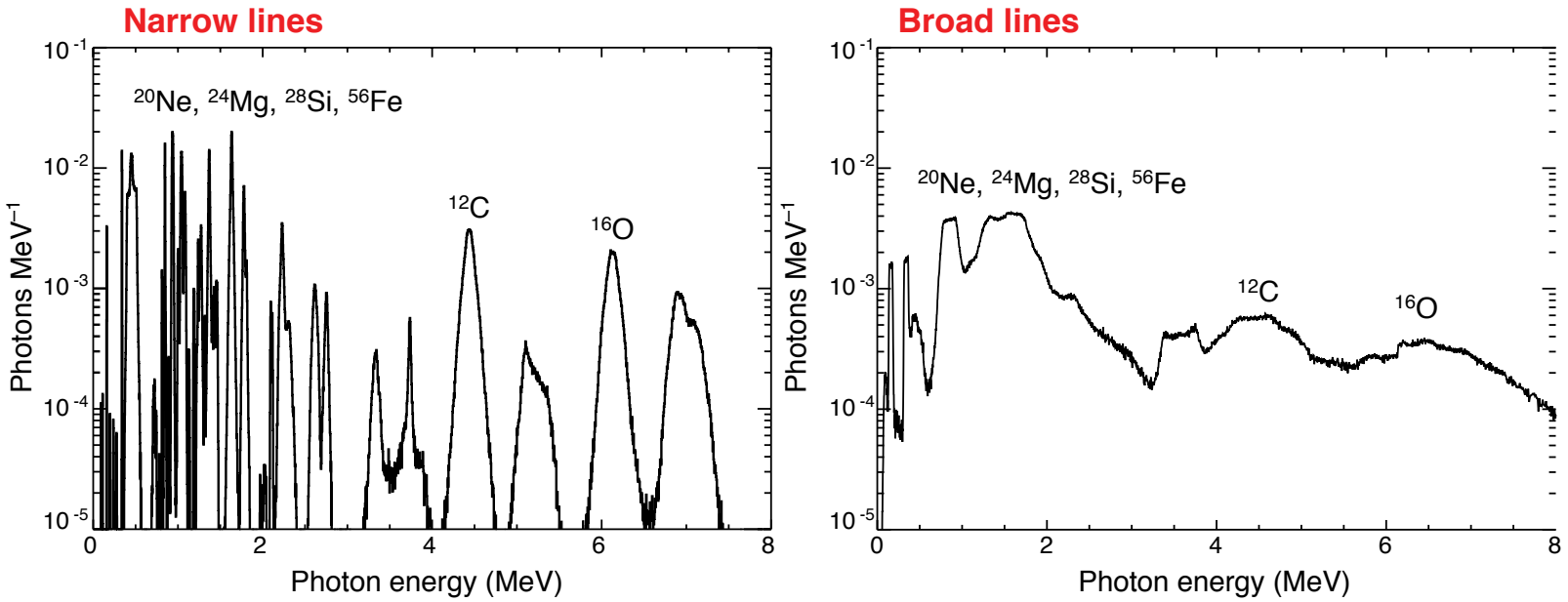

Ambient Composition

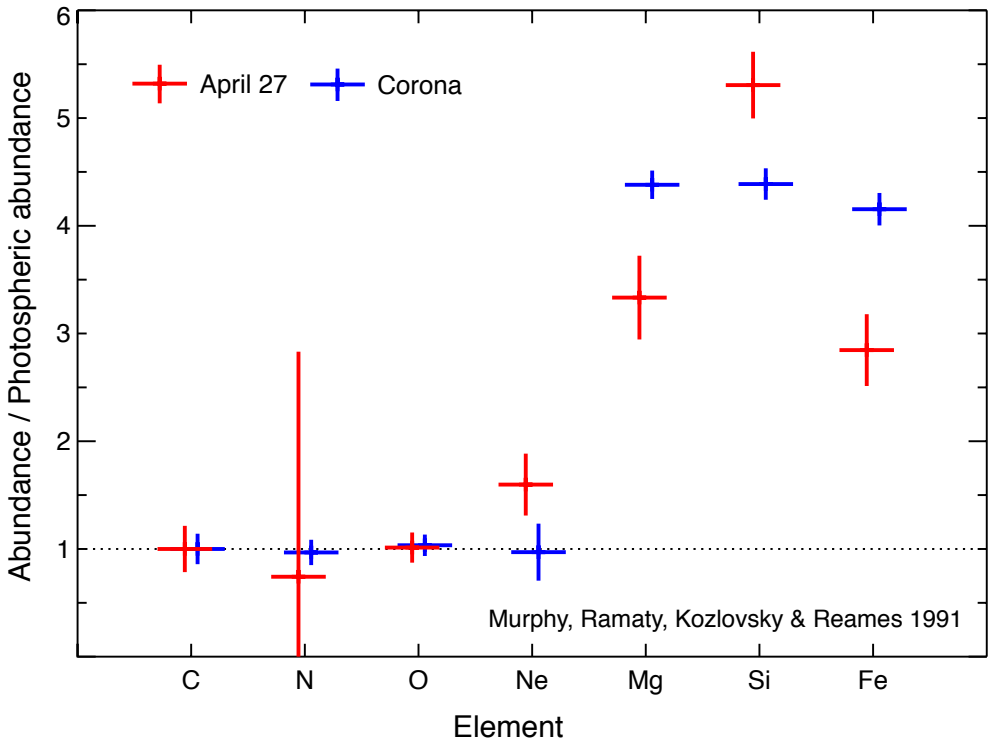

Earlier analyses (Ramaty et al. 1995) found:

The ambient composition is similar to that of the corona (FIP effect).

The Ne abundance appears to be elevated (Ne/O = 0.25 vs. 0.15)

But more recent analyses (Share priv. comm.) found:

The ambient composition is consistent with the photosphere.

The Ne abundance is not elevated.

Accelerated-Ion Composition

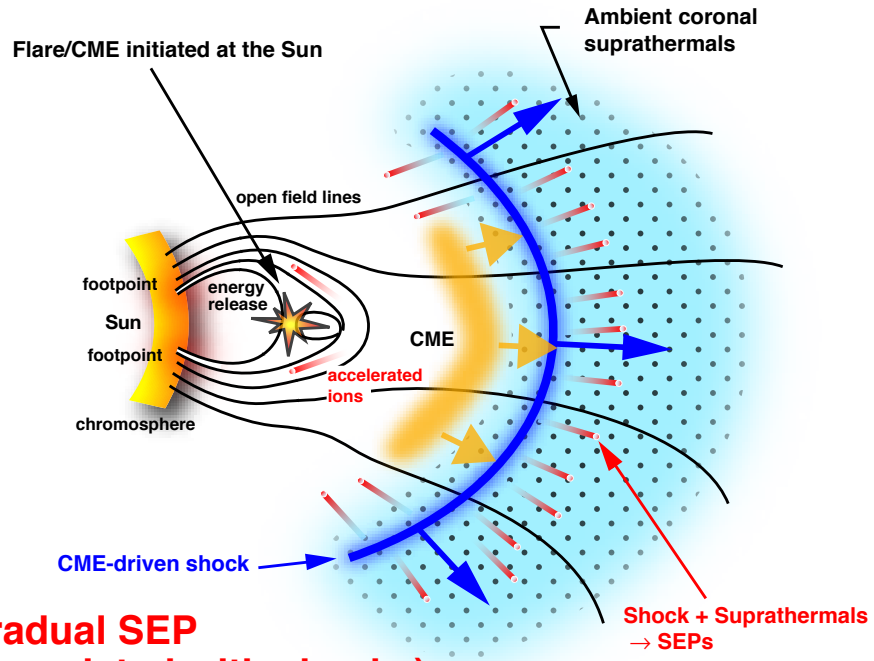

Gradual SEP (associated with shocks)

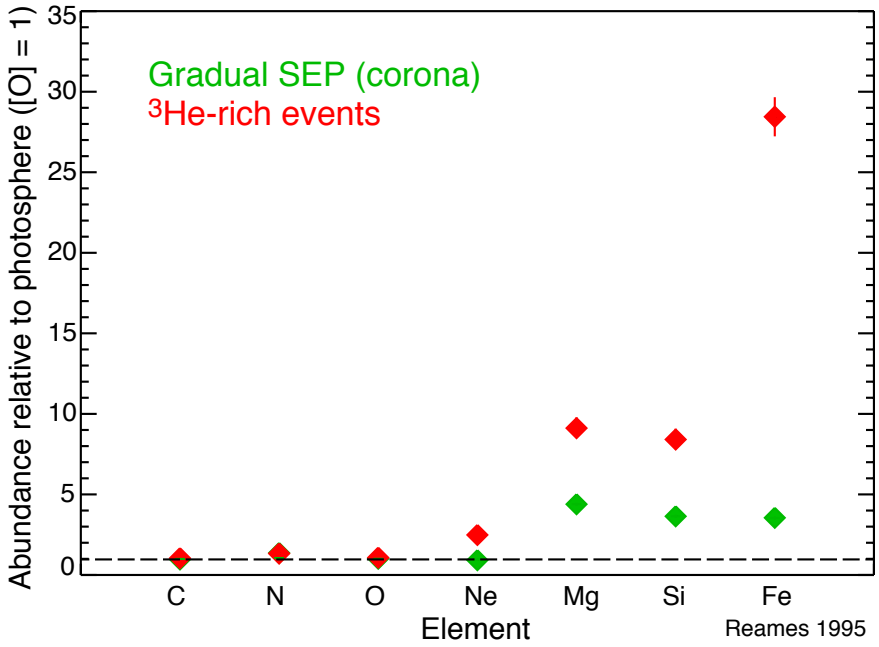

^{3}He-rich impulsive SEP (associated with flares)

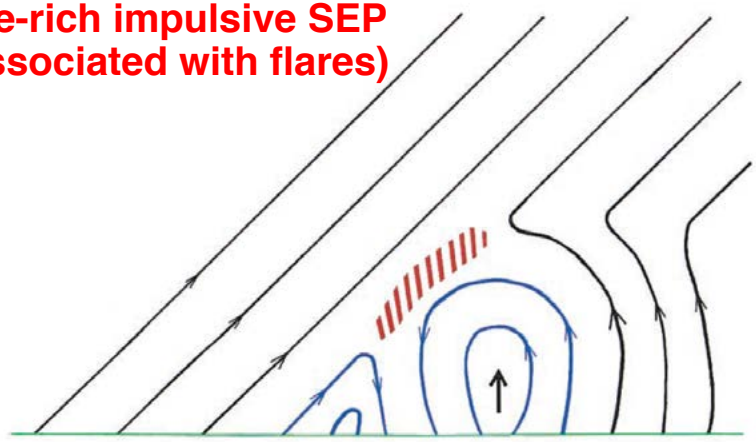

Reames 2002

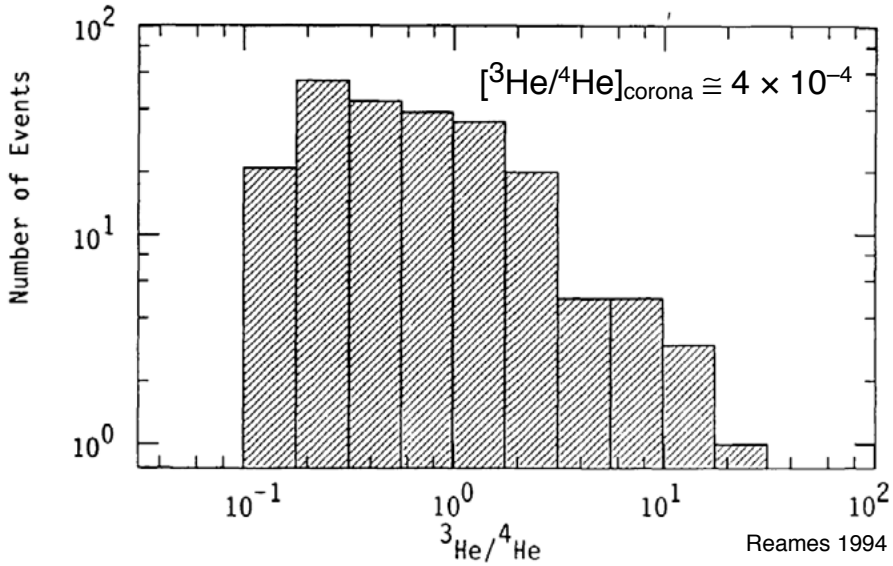

Accelerated-Ion Composition (cont.)

Fitting calculated broad-line spectra to measured spectra directly determines the heavy accelerated-ion composition

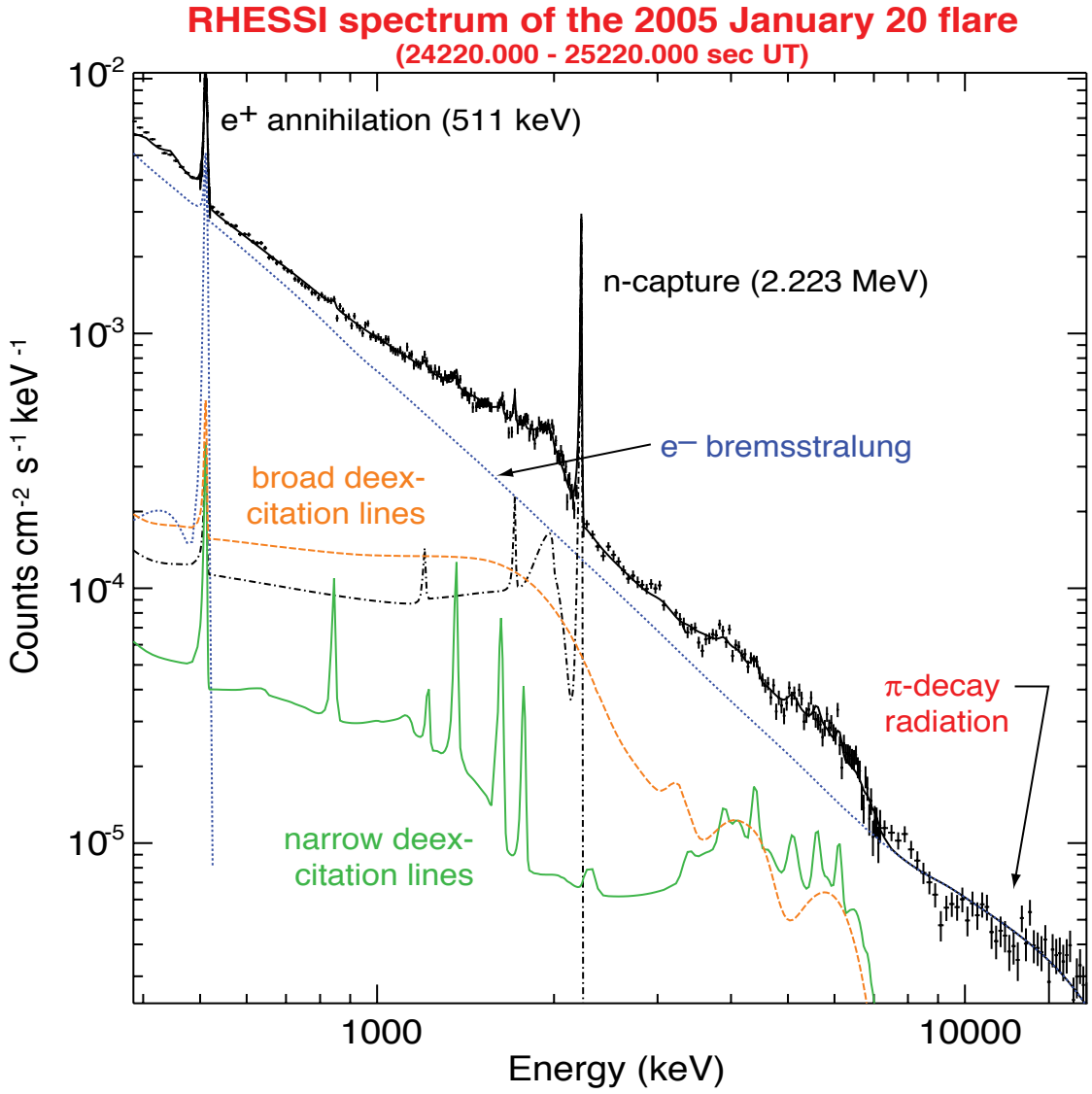

Accelerated-Ion Composition (cont.)

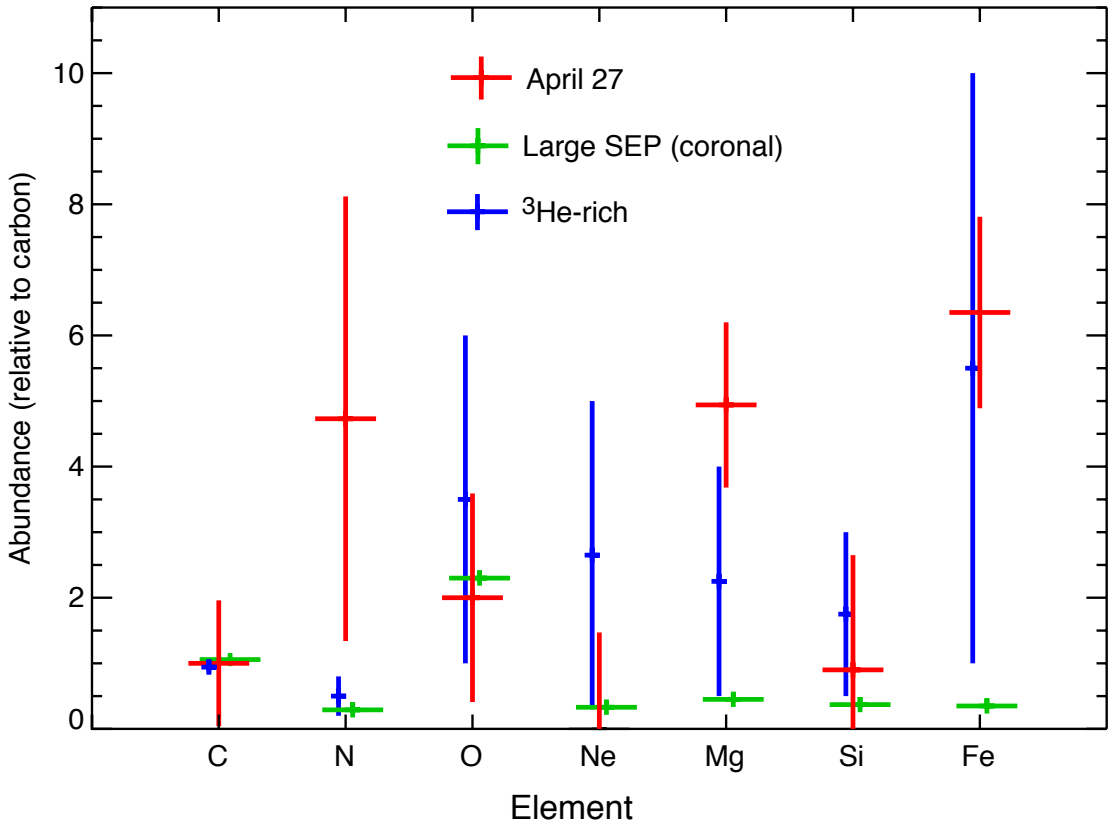

Earlier analyses (Murphy et al. 1991) found:

The accelerated-ion composition may resemble ^{3}He-rich SEP composition.

Conclusion based primarily on the Mg and Fe results.

But more recent analyses (Share priv. comm.) found:

The accelerated-ion composition may be more consistent with a coronal composition, *but* with the heavy/proton ratio larger by a factor of ~2.

Accelerated-Ion Composition (cont.)

Direct determination of the accelerated ^{3}He abundance via ^{3}He deexcitation lines

2.313 MeV line of ^{14}N

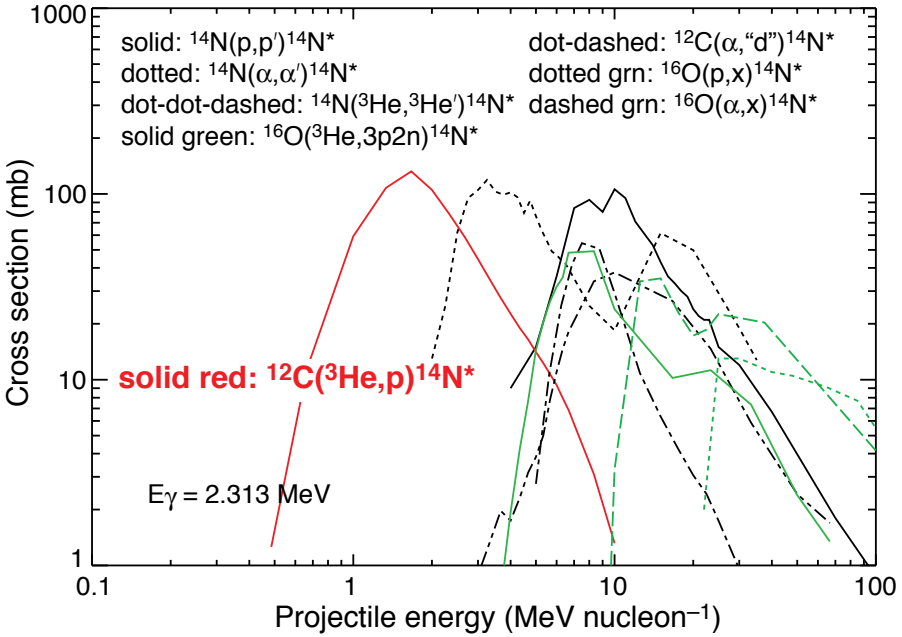

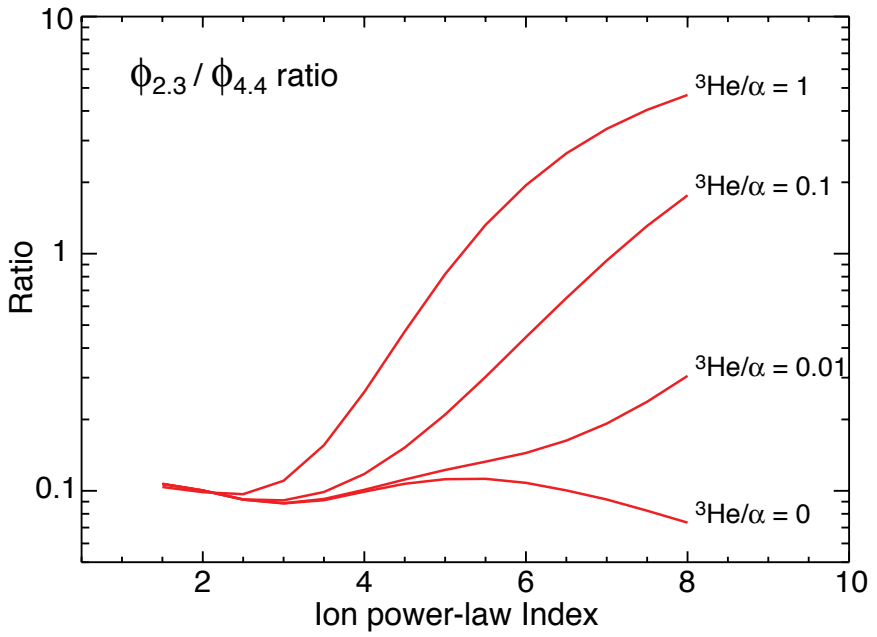

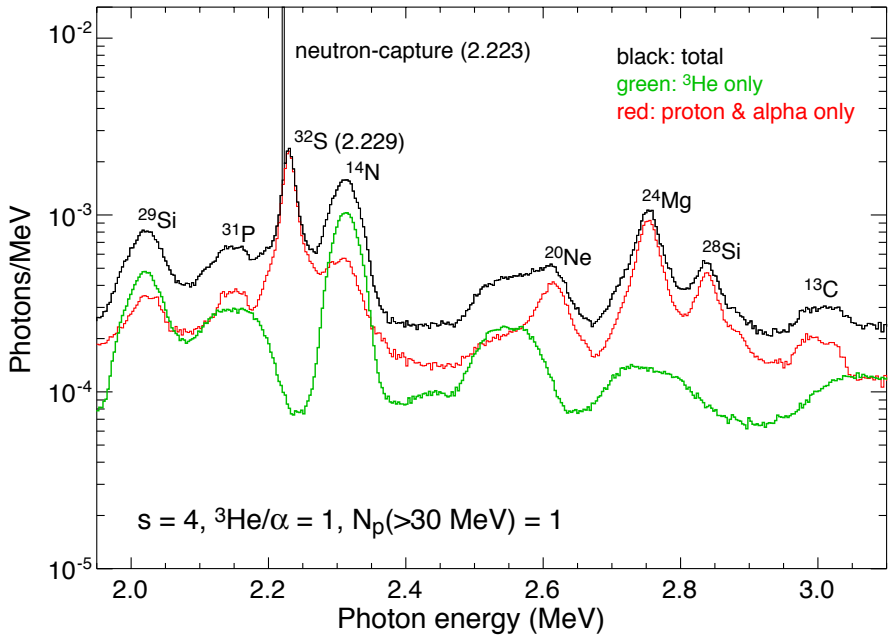

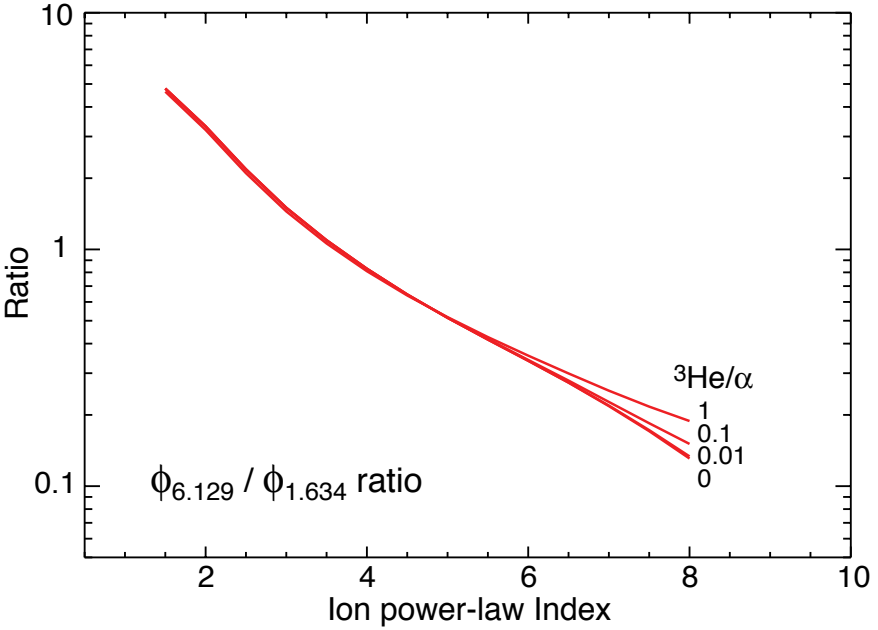

Interacting Accelerated-Ion Angular Distribution

Provides information about ion transport in the flare magnetic loop

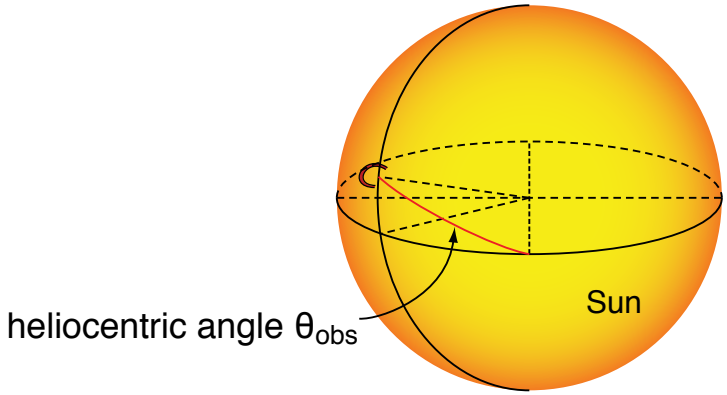

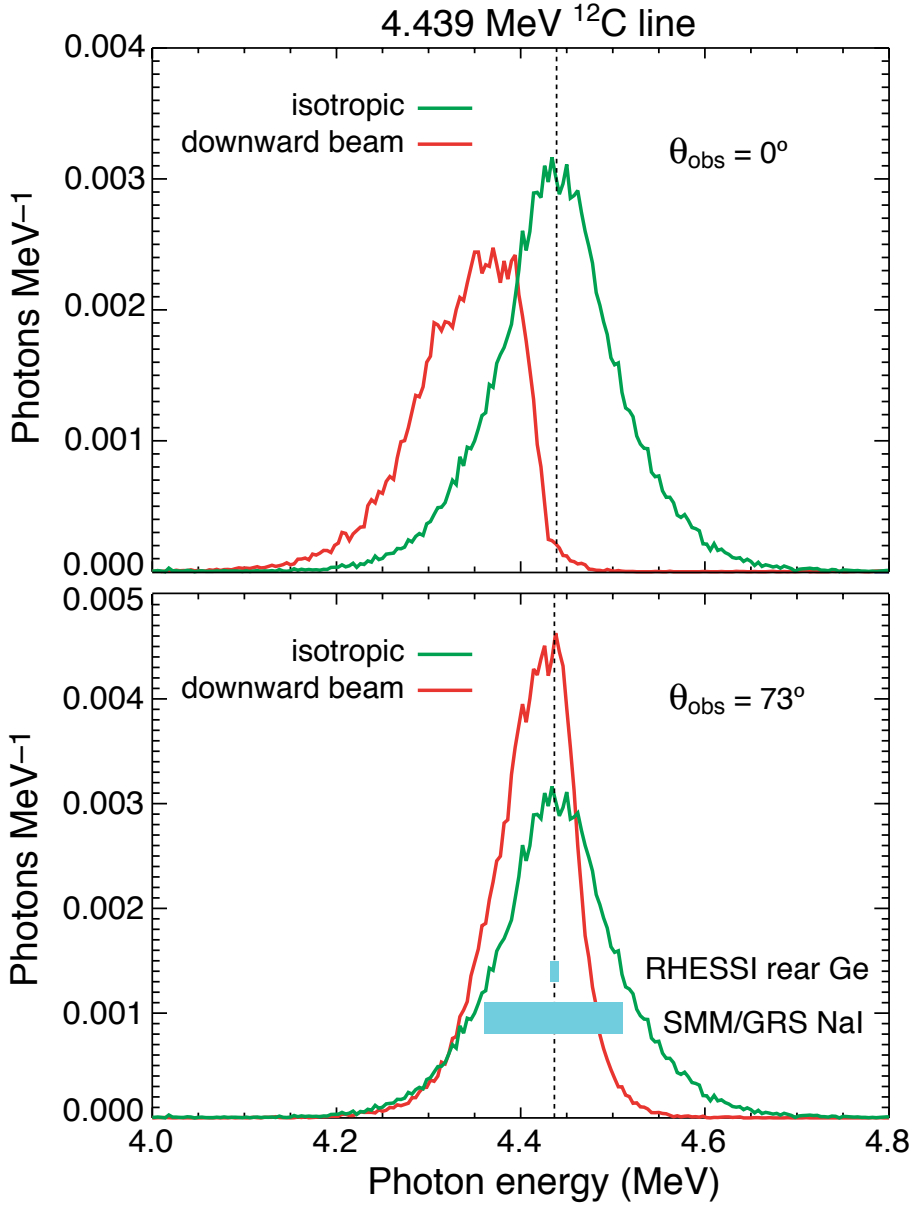

Interacting Accelerated-Ion Angular Distribution (cont.)

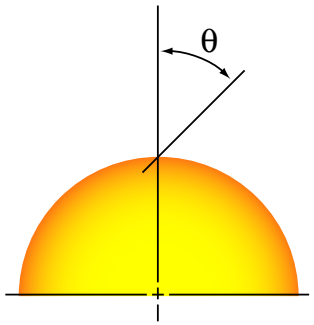

$\mu = \cos(\theta)$

$\mu > 0 \Rightarrow$ upward

$\mu < 0 \Rightarrow$ downward

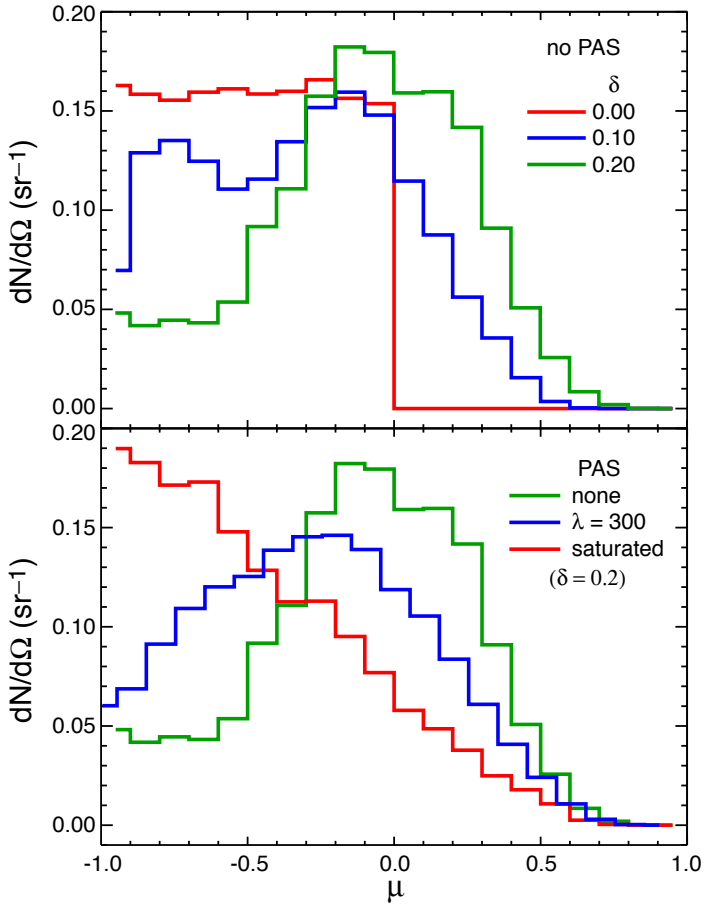

SMM observations (Share, priv. comm.)

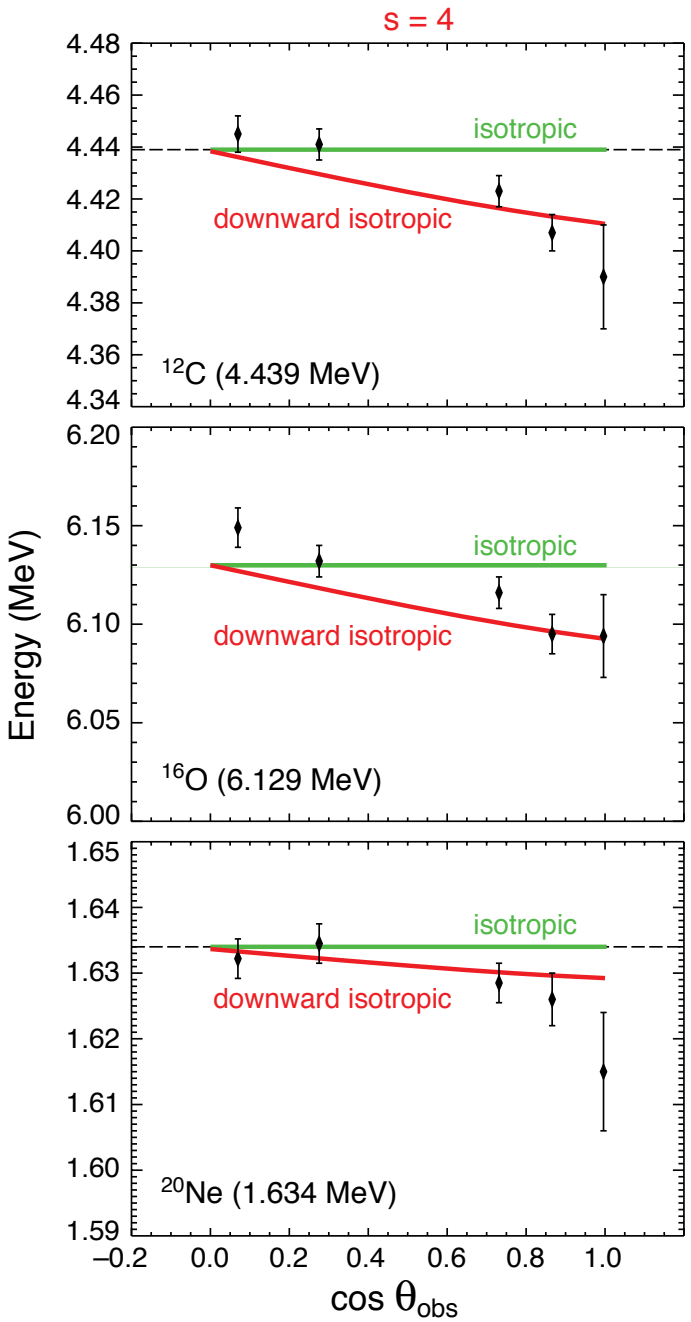

Positron Production and Annihilation

Positron Production

Radioactive positron emitters

$$\left.\begin{matrix} p \\ \alpha \end{matrix}\right\} + {}^{12}C \longrightarrow {}^{11}C + X$$

$$\downarrow_{\tau} \; {}^{11}B + \nu + e^{+}$$

τ (sec)

${}^{16}O\ 9.6 \times 10^{-11}$ ${}^{11}C\ 1800$

Pions

$$\left.\begin{matrix} p + p \\ p + \alpha \end{matrix}\right\} \longrightarrow \pi^{+} \xrightarrow[\tau_{\pi}]{} \mu^{+} + \nu$$

$$\downarrow_{\tau_{\mu}} \; e^{+} + \nu + \bar{\nu}$$

τ (sec)

$\pi^{+}\ 3.8 \times 10^{-8}$ $\mu^{+}\ 2.1 \times 10^{-6}$

Positron Annihilation

1. Direct annihilation with free electrons (daf) or bound electrons (dab) yields two 0.511 MeV photons in rest frame producing a line

2. Positronium (Ps) formation via radiative combination with free electrons (rc) or charge exchange with H and He (ce)

Two possible Ps spin configurations

^{1}Ps $\rightarrow$ 2 511keV photons (a line)

^{3}Ps $\rightarrow$ 3 <511 keV photons (continuum)

Positron Production and Annihilation (cont.)

The annihilation path depends on the ambient density, temperature and ionization fraction

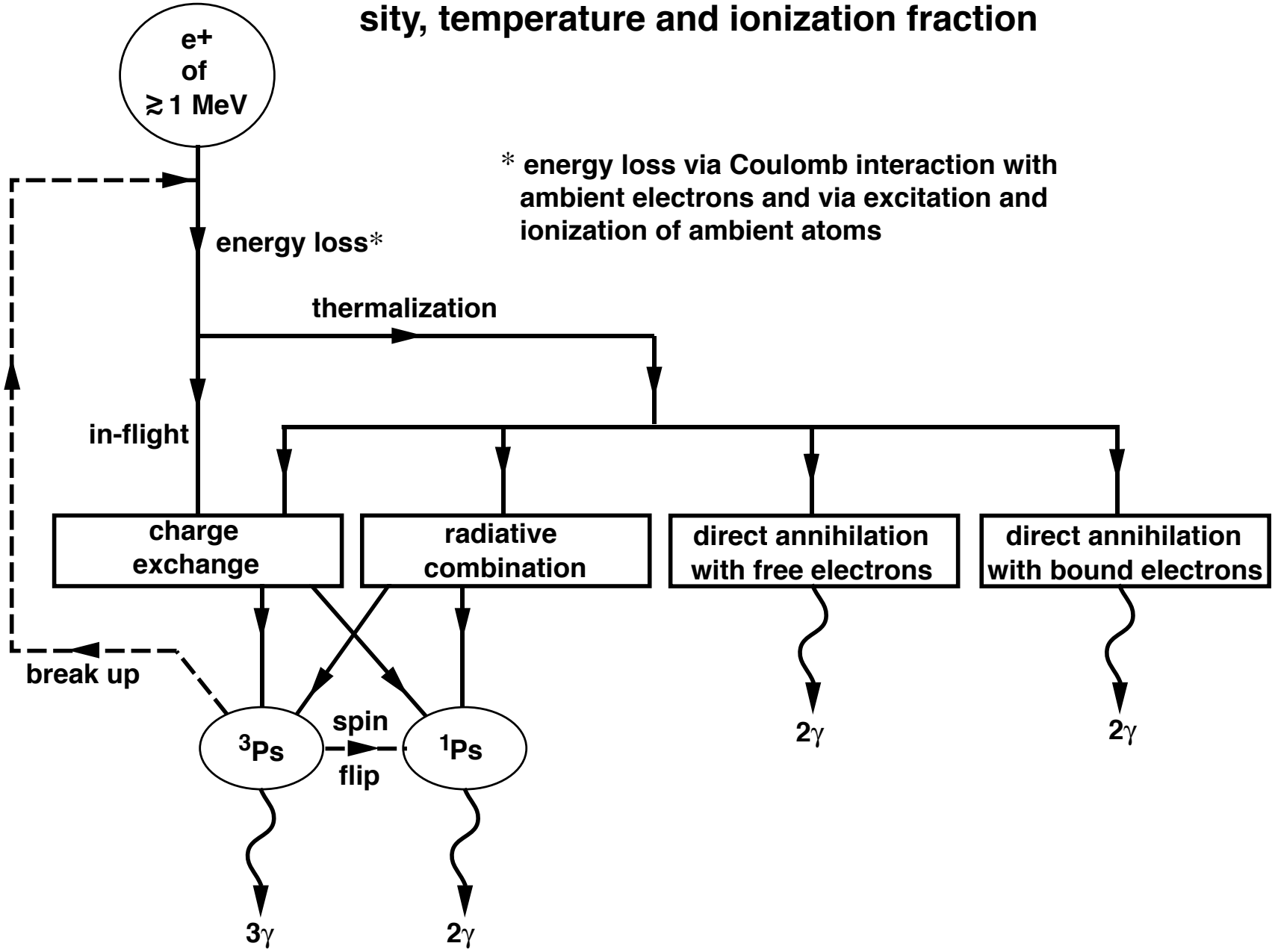

* energy loss via Coulomb interaction with ambient electrons and via excitation and ionization of ambient atoms

Positron Production and Annihilation (cont.)

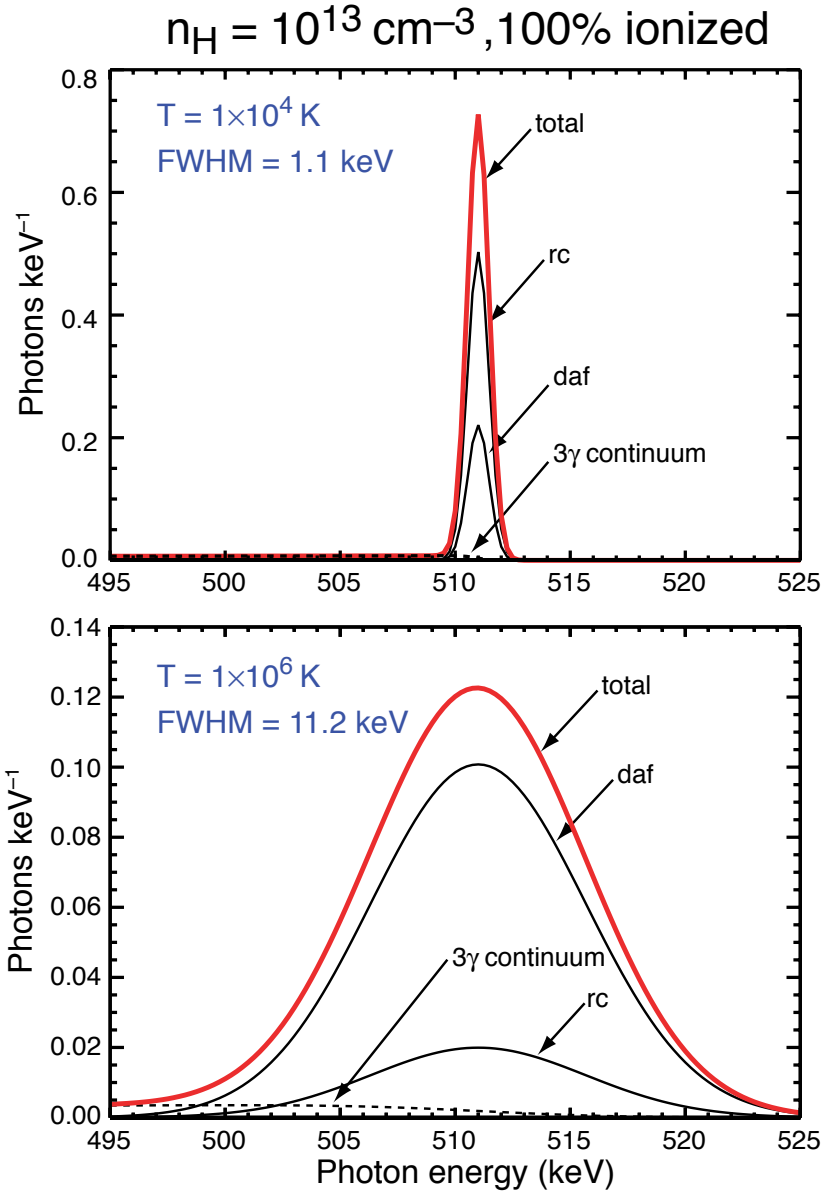

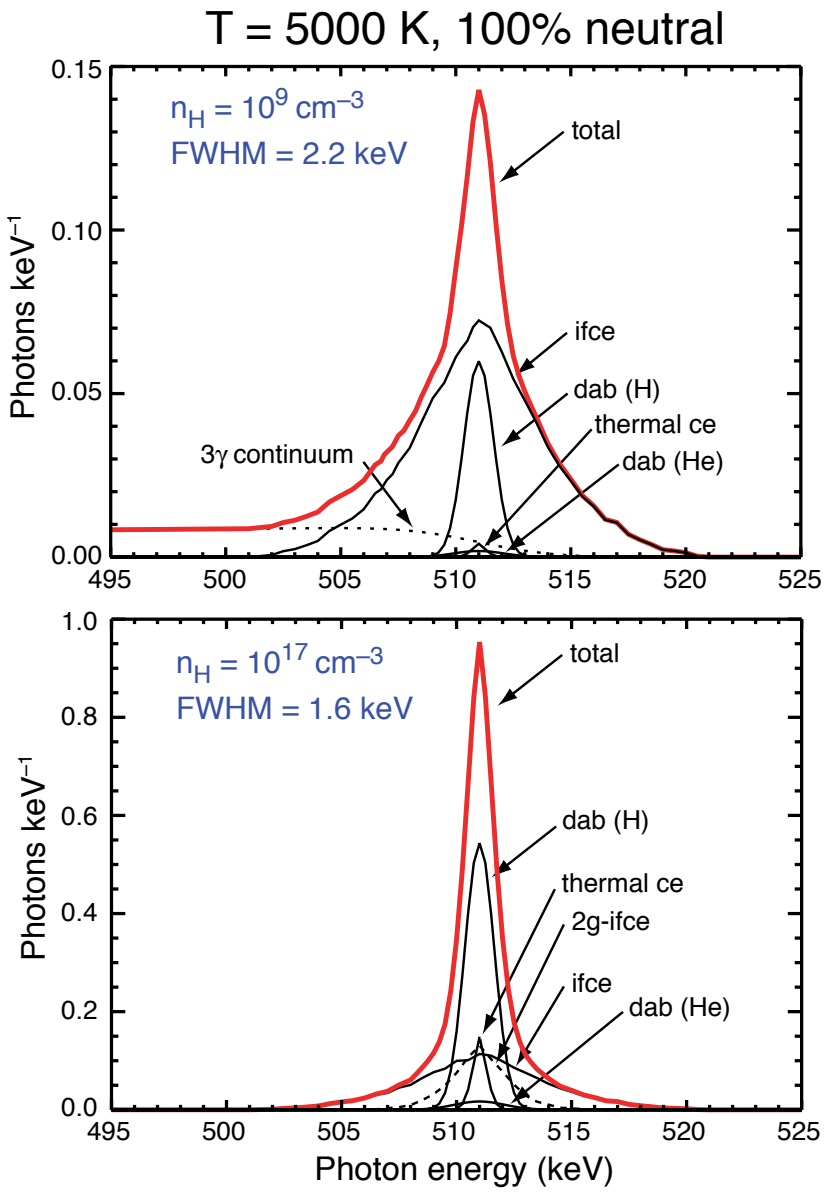

The line shape is NOT Gaussian!

Positron Production and Annihilation (cont.)

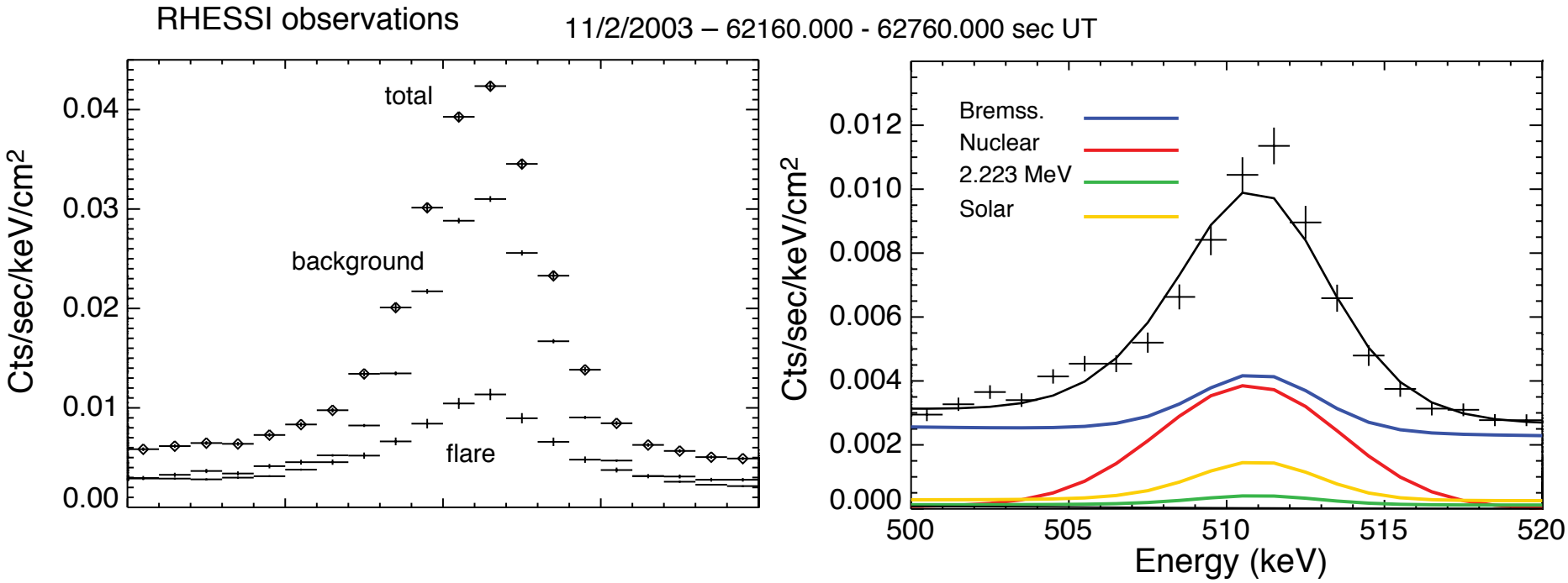

Positron Production and Annihilation (cont.)

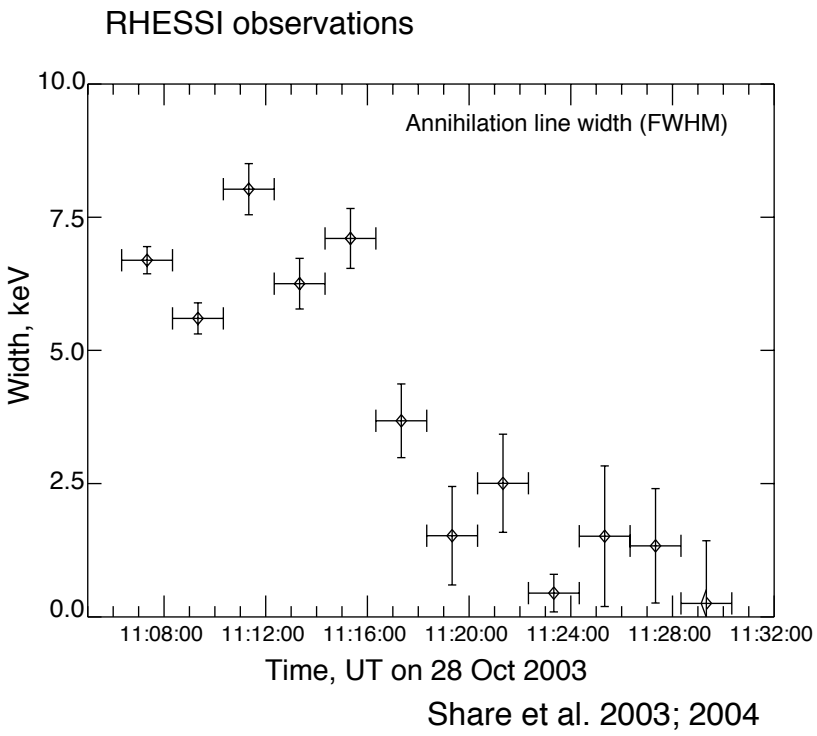

Share et al. 2003; 2004

Broad line: dense, warm, ionized
Narrow line: cool, highly ionized

Neither are consistent with standard atmospheric models.

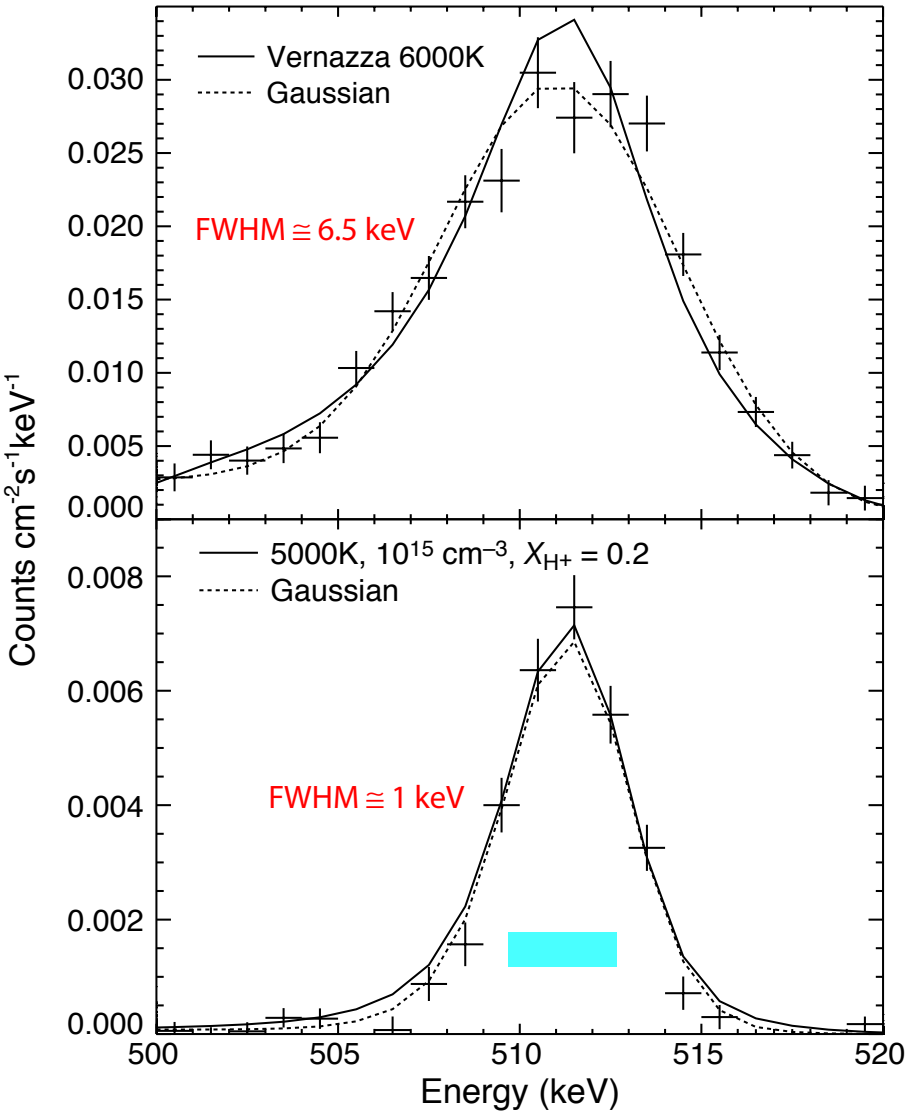

Long-lived Deexcitation Lines

$$p + {}^{12}C \rightarrow {}^{11}C \rightarrow {}^{11}B + \nu + e^{+} \rightarrow \gamma_{511}$$
$$\tau = 1800 \text{ s}$$

$$p + {}^{56}Fe \rightarrow {}^{52}Mn \rightarrow {}^{52}Cr^{*} \rightarrow \gamma_{1434}$$
$$\tau = 21 \text{ m}$$

0.511 MeV positron-annihilation line is strongest

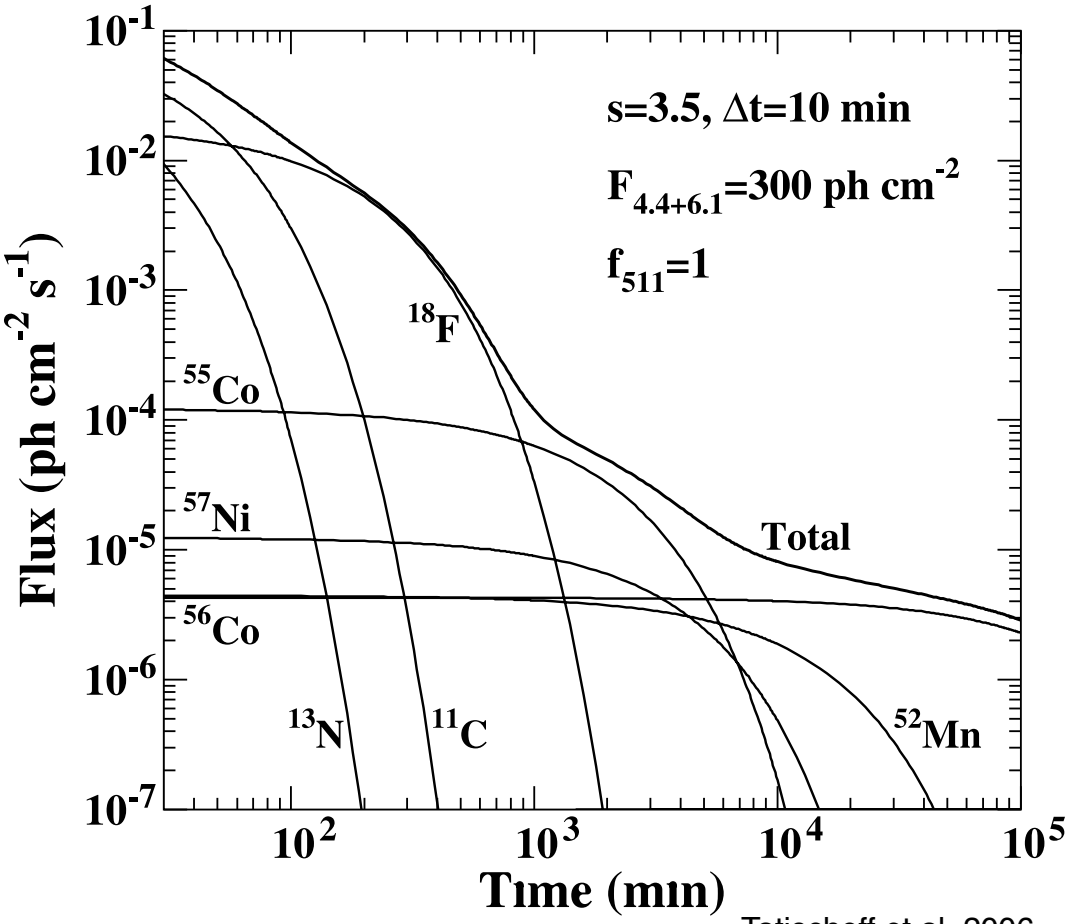

Tatischeff et al. 2006

Long-lived Deexcitation Lines (cont.)

Radioactive X- and Gamma-Ray Line Emitters Ordered by Lifetime

Isotope	Half-Life	Photon Energy (keV) and Intensity (%)
$^{52}Mn^{m}$	21.1 m	1434 (99.8)
^{60}Cu	23.7 m	7.47 (2.5), 826.4 (21.7), 1332 (88.0), 1792 (45.4)
$^{34}Cl^{m}$	32.00 m	146.4 (40.5), 1177 (14.1), 2127 (42.8), 3304 (12.3)
^{63}Zn	38.47 m	8.04 (2.5)
^{49}Cr	42.3 m	4.95 (2.5), 62.3 (16.4), 90.6 (53.2), 152.9 (30.3)
^{56}Mn	2.5789 h	846.8 (98.9), 1811 (27.2), 2113 (14.3)
^{45}Ti	184.8 m	4.09 (2.3)
^{61}Cu	3.333 h	7.47 (12.6), 283.0 (12.2), 656.0 (10.8)
^{43}Sc	3.891 h	372.9 (22.5)
^{44}Sc	3.97 h	1157 (99.9)
^{52}Fe	8.275 h	5.90 (11.2), 168.7 (99.2)
$^{58}Co^{m}$	9.04 h	6.92 (23.8)
^{24}Na	14.9590 h	1369 (100), 2754 (99.9)
^{55}Co	17.53 h	6.40 (6.5), 477.2 (20.2), 931.1 (75.0), 1408 (16.9)
^{57}Ni	35.60 h	6.92 (16.7), 127.2 (16.7), 1378 (81.7), 1920 (12.3)
$^{52}Mn^{g}$	5.591 d	5.41 (15.5), 744.2 (90.0), 935.5 (94.5), 1434 (100)
^{48}V	15.9735 d	4.51 (8.6), 983.5 (100), 1312 (97.5)
^{7}Be	53.22 d	477.6 (10.4)
$^{58}Co^{g}$	70.86 d	6.40 (23.0), 810.8 (99.4)
^{56}Co	77.233 d	6.40 (21.8), 846.8 (99.9), 1038 (14.2), 1238 (66.9), 1771 (15.5), 2598 (17.3)

Tatischeff et al. 2006

Delayed X- and Gamma-Ray Line Fluxes at 3 Hours

Energy (keV)	Parent Nucleus	Line Flux (photons cm^{-2} s^{-1})
511	^{18}F, ^{11}C, ^{55}Co...	6.44×10^{-3}
6.92	$^{58}Co^{m}$, ^{57}Ni	1.59×10^{-4}
931.1	^{55}Co	1.07×10^{-4}
1369	^{24}Na	6.98×10^{-5}
2754	^{24}Na	6.97×10^{-5}
846.8	^{56}Co, ^{56}Mn	4.31×10^{-5}
1434	$^{52}Mn^{m}$, $^{52}Mn^{g}$	2.97×10^{-5}
477.2	^{55}Co	2.89×10^{-5}
1408	^{55}Co	2.42×10^{-5}
1378	^{57}Ni	2.20×10^{-5}
6.40	^{55}Co, ^{56}Co, $^{58}Co^{g}$	1.59×10^{-5}
1238	^{56}Co	1.51×10^{-5}
935.5	$^{52}Mn^{g}$	1.40×10^{-5}
744.2	$^{52}Mn^{g}$	1.33×10^{-5}
7.47	^{61}Cu, ^{60}Cu	1.11×10^{-5}
283	^{61}Cu	1.06×10^{-5}

$\phi_{4.4+6.1} = 300$ ph cm^{-2} s^{-1}

s = 3.5

Tatischeff et al. 2006

Fermi/LAT Observations

Pion-decay emission from >300 MeV protons

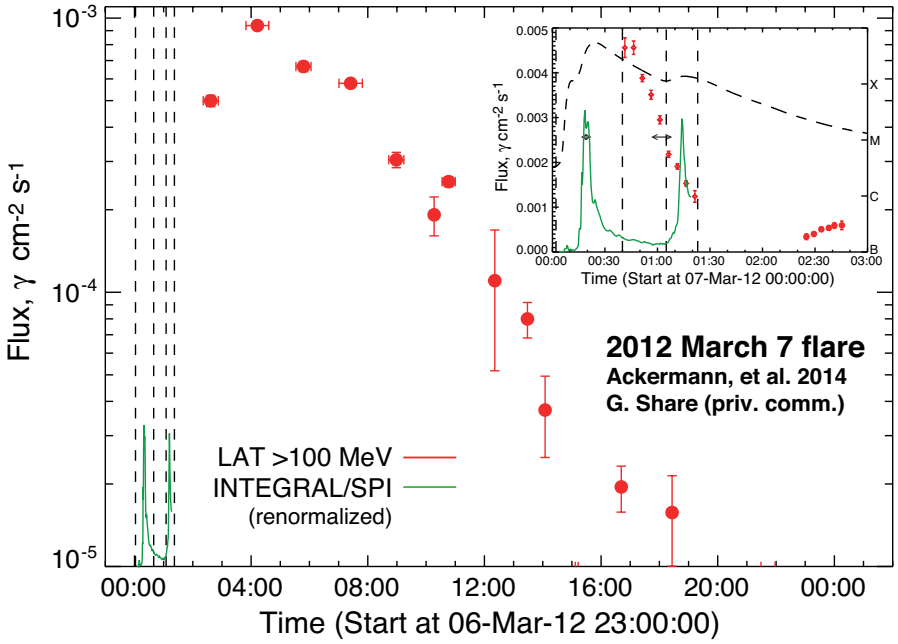

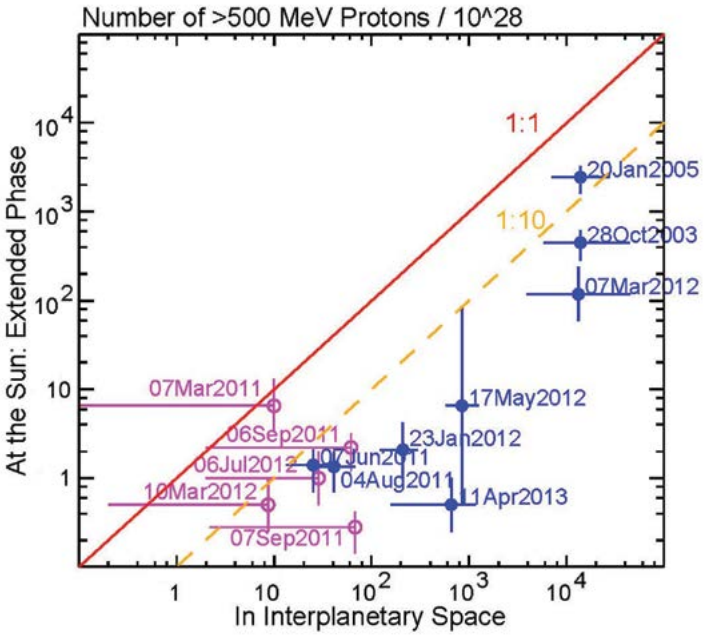

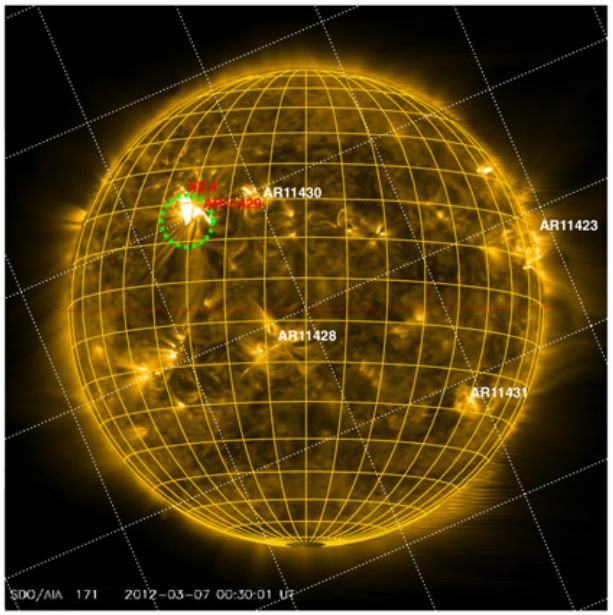

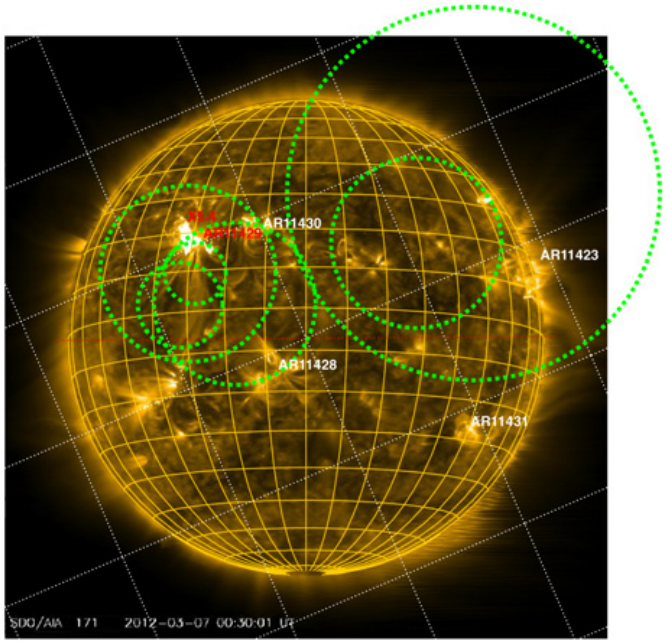

Ajello et al. 2014

Fermi/LAT pion-decay emission from a flare located beyond the solar limb. (Pesce-Rollins 2015)

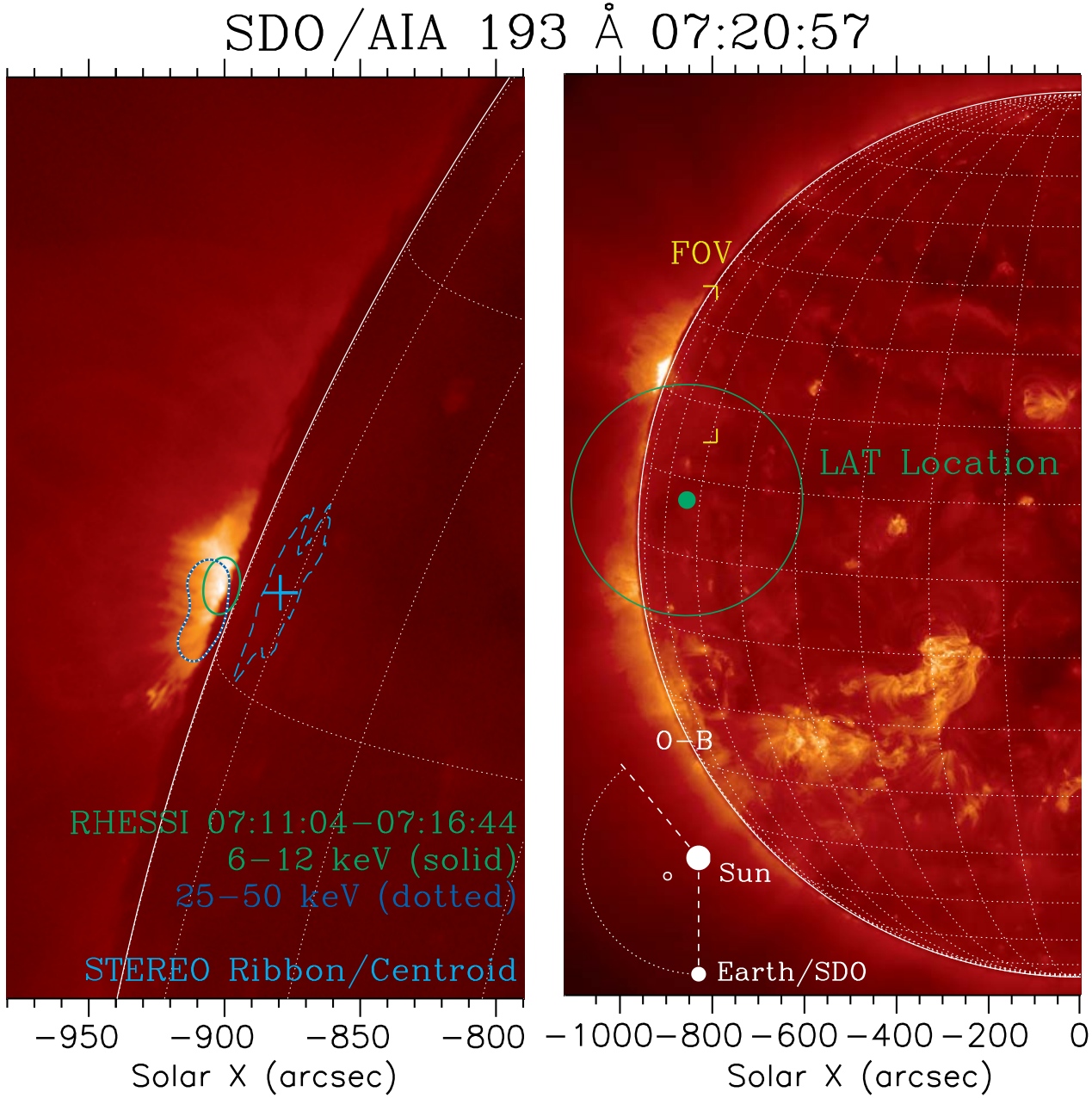

Fermi/LAT Observations (cont.)

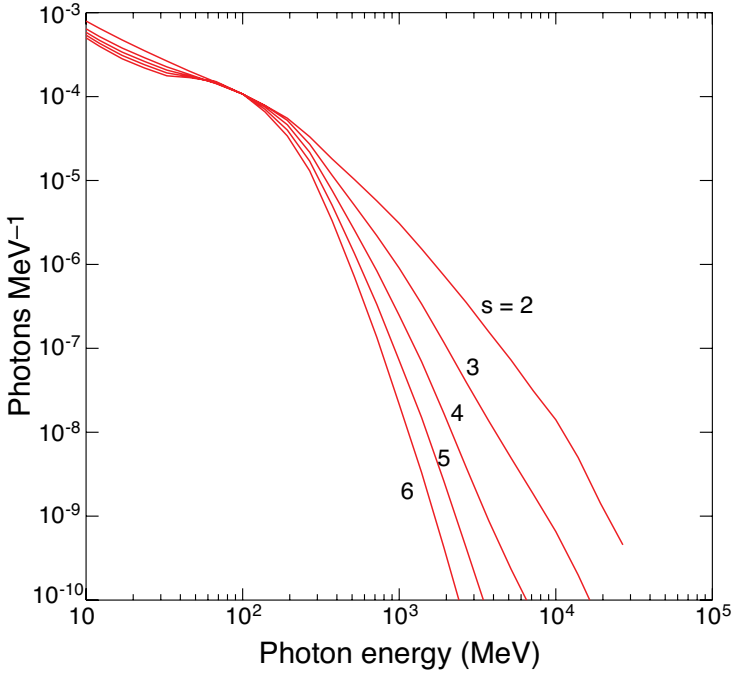

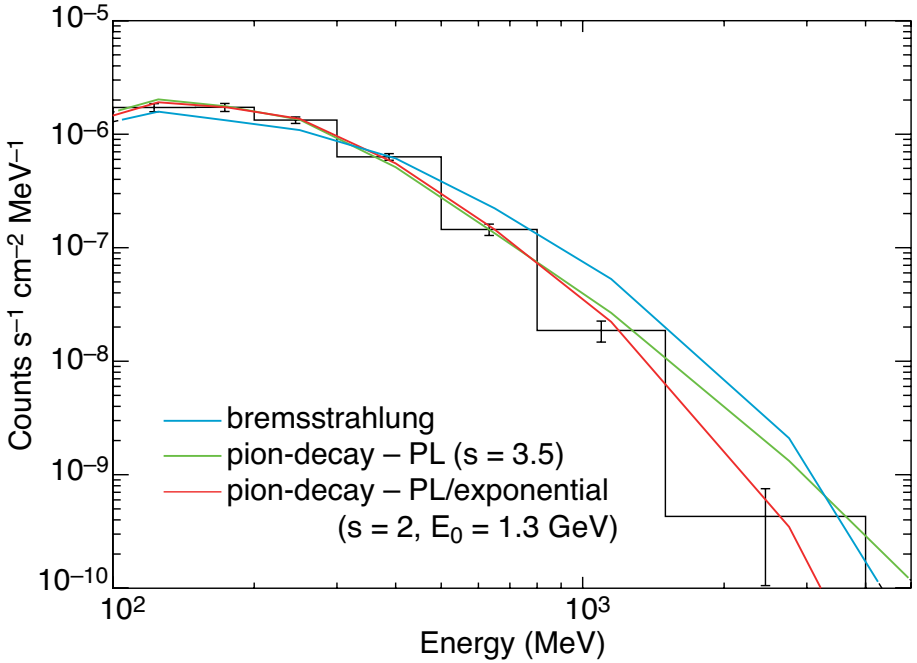

Provides both the shape of >300 protons and their number

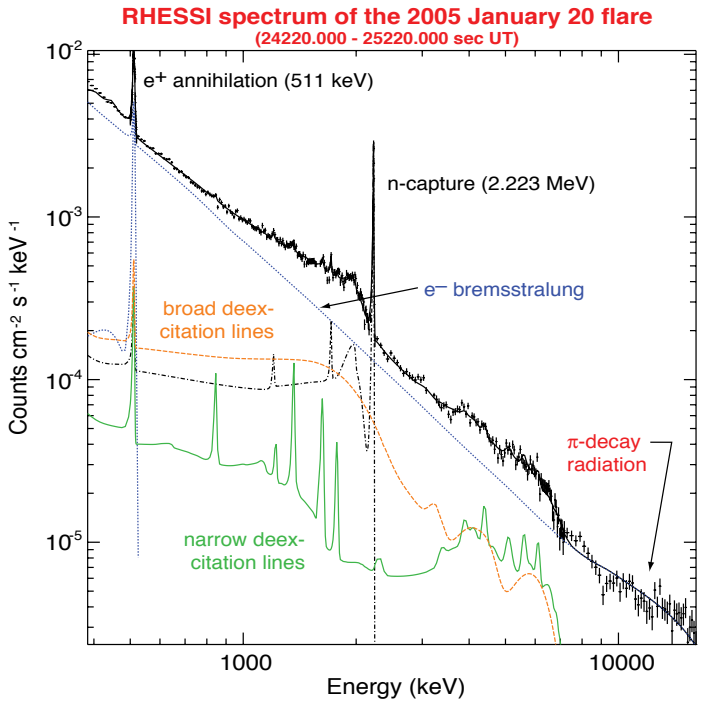

Observations up to only 20 MeV can provide the number of interacting >300 MeV protons but not the spectral shape

Neutron Observations

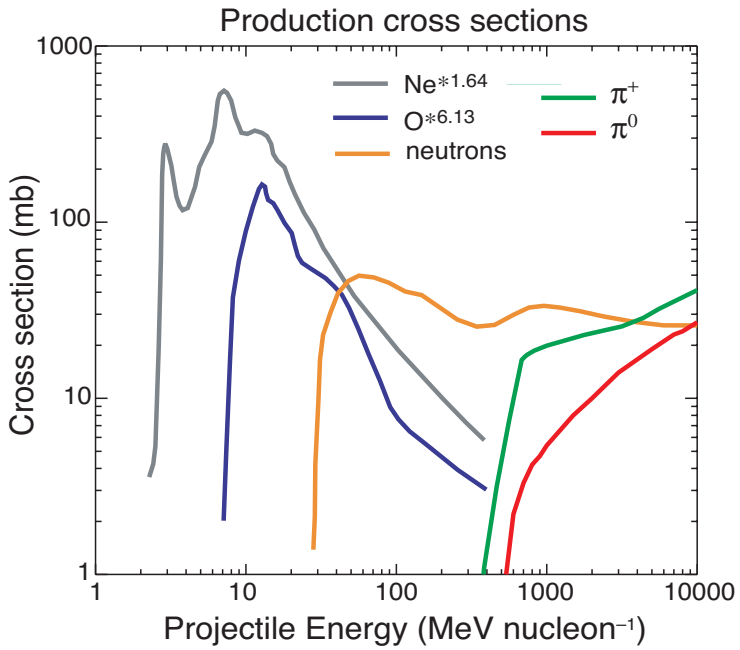

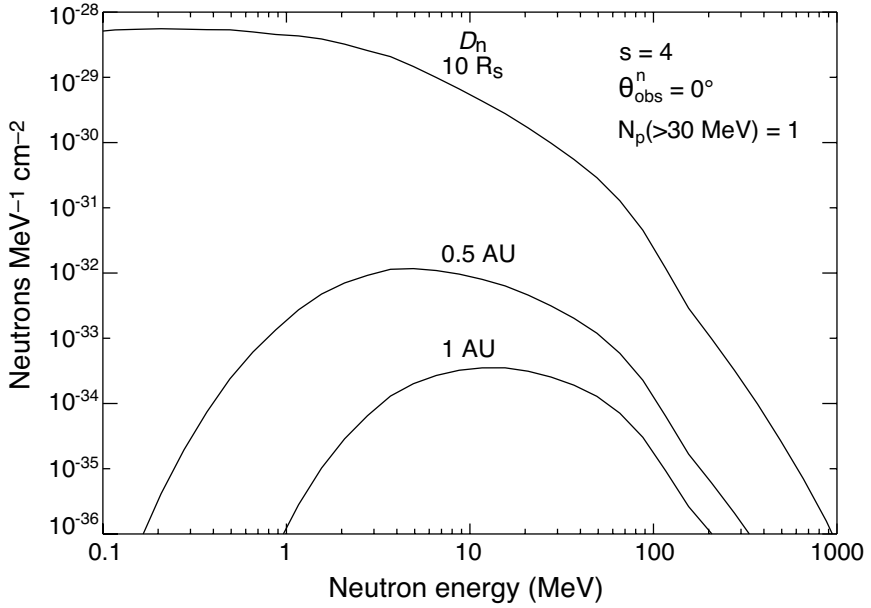

$$R = \frac{\phi_{1-10\ \text{neutrons}}(D_n)}{\phi_{2.223\ \text{MeV}}(D=1\ \text{AU})}$$

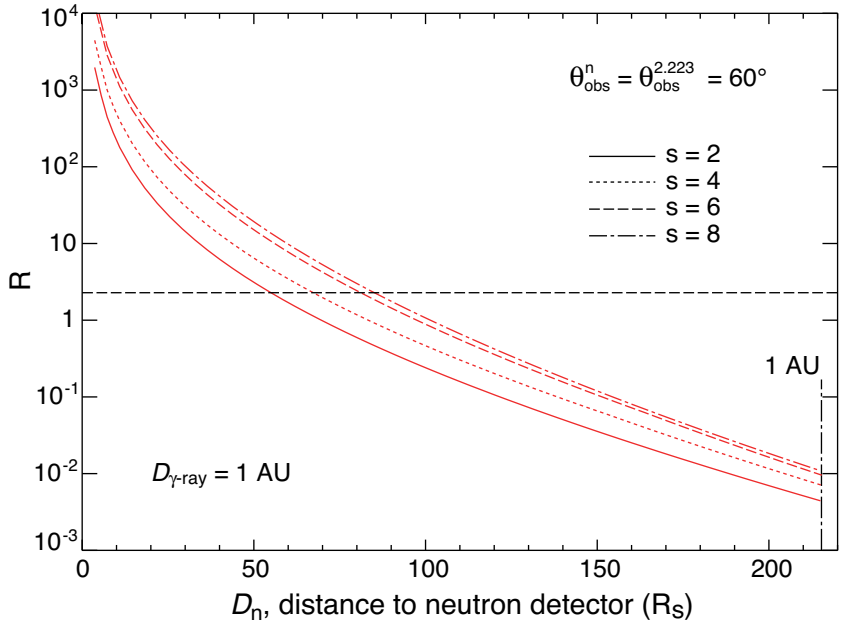

Electron Bremsstrahlung

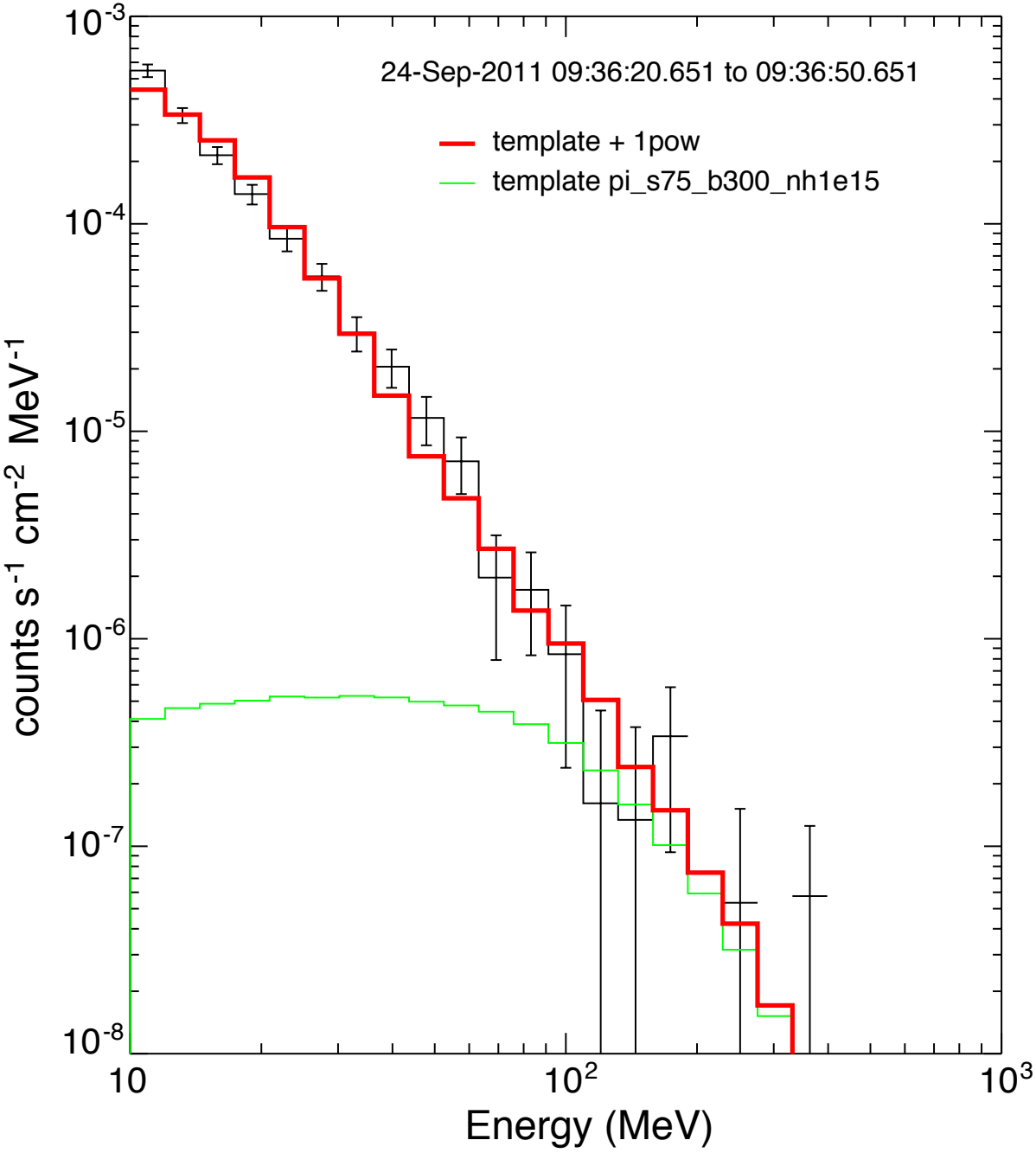

Performance parameter	Goal value
Field-of-view (FWHM, deg)	~1°
Angular resolution (FWHM)	~5 arc min ~0.5 arc min for foot pts
Spectral resolution ($\Delta E/E$ @ Energy)	1 – 2% at 5 MeV
Line sensitivity (@ Energy) ($cm^{-2}.s^{-1}$, 3 σ , 1 Ms)	~10^{-6} at 1 MeV
Timing performance	~1 ms
Polarimetric capability (Minimum Polarization Fraction)	10% in 10 s